Available online at www.sciencedirect.com
ScienceDirect
Ceramics International 35 (2009) 1991–1997
CERAMICS INTERNATIONAL
www.elsevier.com/locate/ceramint

Fabrication and characterization of bioactive glass (45S5)/titania biocomposites

Hanan H. Beherei, Khaled R. Mohamed *, Gehan T. El-Bassyouni

National Research Centre, Biomaterials Department, Behoos Street, Dokki, Giza, Egypt

Received 21 August 2007; received in revised form 27 September 2008; accepted 28 October 2008
Available online 17 November 2008

Abstract

Bioactive glass (BG) (45S5) has been used successfully as bone-filling material in orthopedic and dental surgery but its lean mechanical strength limits its applications in load-bearing positions. Approaches to strengthen these materials decreased their bioactivity. In order to realize the optimal matching between mechanical and bioactivity properties, bioactive glass (45S5) was reinforced by introducing titania (TiO_2) in anatase form and treated at 1000 °C to form new bioactive glass/titania biocomposites. The prepared biocomposites were assessed by XRD, FT-IR, mechanical properties and SEM. The results verified that the increase of titania percentage to BG powder enhanced gradually the mechanical data of the prepared biocomposites. SEM and FT-IRRS confirmed the presence of a rich bone-like apatite layer post-immersion on the composite surface. It has been found that the new BG/titania biocomposite materials especially those containing high content of titania have high bioactivity properties and compressive strength values comparable to cortical bone. Therefore, these biocomposite materials are promising for medical applications such as bone substitutes especially in load-bearing sites.

Keywords: Titania; Bioactive glass; Biocomposites; Bone implants; SBF; SEM

1. Introduction

Artificial implants, such as the total hip replacement, are successful for a limited time, but all orthopedic implants lack three of the most critical characteristics of living tissues: (a) the ability to self-repair; (b) the ability to maintain a blood supply; and (c) the ability to modify their structure and properties in response to environmental factors such as mechanical load. A recent study showed that 24% of charnley hip operations required revision surgery [1]. Since the discovery of ''Bioglass'' by Hench in the late sixties [2], many bioactive materials (e.g. glasses, sintered HA, glass–ceramics, composites), which exhibit the ability to bond to living bone through a hydroxyapaptite (HA) layer formed onto their surfaces, have been synthesized and developed for medical applications [3]. The mechanism of HA formation is widely accepted that involves dissolution of calcium ions from the surface of bioactive materials, which increases the super-saturation in the surrounding fluid, with respect to HA components. The simultaneous dissolution of silicates results in the formation of silanol groups on material's surface, which are essential for nucleation sites leading to HA formation [4]. However, bioglass implants present critical drawbacks in their low mechanical properties and this causes great limitations to their use for load-bearing sites. For this reason, bioglass parts often coupled with tougher material, providing thus their excellent surface properties without a great loss in the bioactivity of the bioglass [5,6].

The apatite can be formed biomimetically on bioactive materials even in simulated body fluid with ion concentrations. TiO_2 has a tendency to adsorb water at the surface, resulting in the formation of titanium hydroxide groups. The basic Ti–OH groups were reported to induce apatite nucleation and crystallization in SBF [7]. The production of composite materials has proven to be suitable solutions for improving the mechanical properties of weaker materials. Ceramic matrix biocomposites were reinforced by introducing another tough phase [8] Al_2O_3, ZrO_2, and other. The choice or the design of the best materials for a specific application plays an important role in the feasibility of high

* Corresponding author. Fax: +2 02 33370931.
E-mail address: kh_rezk@yahoo.com (K.R. Mohamed).

0272-8842/$34.00
doi:10.1016/j.ceramint.2008.10.014

performance components. Among the most promising materials and already a reality in many applications are advanced whose properties in specific fields other classes of materials [8] seldom match.

Therefore, the present work is concerned with the preparation and characterization of novel biocomposites containing bioactive glass (BG) and titania. Also, these biocomposites were followed in simulated body fluid (SBF) to verify the formation of a bone-like apatite layer on their surfaces by using in vitro test, FT-IR and SEM techniques.

2. Experimental

2.1. Preparation of the BG/titania composites

Bioactive glass (BG) (45S5) having the following composition (45% SiO_2, 24.5% Na_2O, 24.5 CaO, 6% P_2O_5) reagent-grade chemicals [9], all in weight% was prepared by melting at 1325 °C in a covered platinum rhodium crucible, homogenized for 2 h, cast, crushed, and sieved to a particulate size of 100–300 μm. The BG powder is mixed in weight ratios 75, 50 and 25% with TiO_2 powder (anatase form, BDH, England), compacted at 1200 MPa pressure into cylindrical samples (1 cm × 1 cm) and fired at 1000 °C to prepare the composites as shown in Table 1. The TiO_2 has particle size equal to d_{50} = 1.5 μm and d_{90} = 2.7 μm and the size of particle was measured by particle size analyzer (Fritsch analystt 22, Germany).

2.2. Characterization of composites

The level of crystallinity of the prepared composites was studied by X-ray powder diffraction (XRD) operating at 40 kV and 25 mA, using Cu K radiation and Ni filter, scanned at 2°/min. Fourier-transform infrared spectroscopy (FT-IR) was used in the wave number range of 4000–400 cm^{-1} to support, to verify the XRD findings, and to provide evidence of ionic substitution.

2.3. Mechanical testing

The composites were tested to determine the effect of filler on mechanical properties. Compressive strength was measured using tensile testing machine, Zwick Z010, Germany. The average value for each test was taken for three samples to verify the results. The shape of sample was cylindrical (1 cm × 1 cm), load cell was 10 kN and crosshead speed was 10 mm/min.

Table 1
Chemical composition of the prepared composites.

Samples	Molar ratio		Weight ratio (%)	
	BG (45S5)	TiO_2	BG (45S5)	TiO_2
T1	3	1	75	25
T2	1	1	50	50
T3	1	3	25	75

2.4. Bioactivity behavior

Control is simulated body fluid (SBF) which contains ions similar to those in human blood plasma (Table 2) and it was prepared by dissolving reagent grade: NaCl (8.035 g), $NaHCO_3$ (0.355 g), KCl (0.225 g), $K_2HPO_4{\cdot}3H_2O$ (0.231 g), $MgCl_2{\cdot}6H_2O$ (0.311 g), $CaCl_2$ (0.292 g) and Na_2SO_4 (0.072 g) in ion exchanged distilled water (1 l). The solution was buffered at pH 7.4 with Tris (hydroxymethylaminomethane) ($(CH_2OH)_3CNH_2$) (6.118 g) and 1 M hydrochloric acid (HCl) (39 ml).

Therefore, the bioactivity of an artificial biomaterial can be evaluated by examining the formation of apatite on its surface in SBF [10]. SBF is prepared to have ionic concentration nearly equal to that of human blood plasma [11]. After the immersion periods end, the solutions were analyzed by spectrophotometer (UV-2401PC, UV-VIS Recording spectrophotometer, Shimadzu, Japan) using biochemical kits (Techo Diagonstic, USA) to detect the total calcium ions $(Ca)^{2+}$ at λ = 570 nm and phosphate ions (PO_4^{3-}) concentration at λ = 675 nm. The immersed specimens were removed from the SBF solution then repeatedly rinsed using de-ionized water and dried. FT-IR and micro-structural feature of the composites pre- and post-immersion in SBF for 4 days at 37 °C were carried out.

3. Results and discussion

3.1. Characterization

3.1.1. Phase analysis

X-ray powder diffraction data of the prepared biocomposites are shown in Fig. 1. The patterns of T1 composite of high % of BG content do not show any peaks for BG due to its amorphous nature and because the intensity of titania peaks is very weak denoting lower content of titania in the T1 composite. These peaks are recorded at d (Å) = 3.24, 2.99 and 2.61 forming calcium titanium silicate [Ca Ti (SiO_5)] compound (Card No.: 73-2066) and proving interaction between TiO_2 and BG powders. For T2 composite containing equal amount of the two powders, Fig. 1 shows the increase of the intensity of calcium titanium silicate oxide peaks denoting more reaction produced between the BG and TiO_2 [12] as well as the appearance of some peaks of titania (rutile form) at d (Å) = 2.49, 2.18, 2.06, 1.68 and 1.62 (Card No.: 04-0551) as a result of the conversion of anatase to rutile form that are not reacted with BG powder. In this domain, anatase transforms into rutile form at any temperature between 600 and 1000 °C [13]. For T3 composite, Fig. 1 shows the increase of intensity of Ca Ti (SiO_5)/TiO_2 peak at d (Å) = 3.25 with disappearance of the peaks at d (Å) = 2.99.

Table 2a
Ion concentrations of SBF solution in comparison with those of human blood plasma concentration in mM.

	Na^+	K^+	Ca^{2+}	Mg^{2+}	HCO_3^-	Cl^-	HPO_4^{2-}	SO_4^{2-}
Blood plasma	142.0	5.0	2.5	1.5	27.0	103.0	1.0	0.5
SBF	142.0	5.0	2.5	1.5	4.2	148.0	1.0	0.5

Table 2b
The mechanical data of the prepared composites and standard errors.

Sample	Three values for each sample	Compressive strength (MPa) (average value)	Standard errors (%) of compressive strength for the tested samples ($n = 3$)
T1	38.96, 34.75, 36.90	36.87	2.10
T2	71.20, 73.40, 72.33	72.31	1.10
T3	121.1, 122.7, 123.1	122.31	1.06
Cortical bone	–	100–230 (Kokubo et al. [8])	–

The peaks of rutile increased and became almost four times compared to those in T2 composite as a result of the highest titania content in the BG/titania composite proving the presence of part of titania powder which does not react with BG powder and converts completely to the rutile form.

3.1.2. FT-IR assessment

Fig. 2 shows the FT-IR spectra of titania (T), bioactive glass (G), and their biocomposites (T1, T2 and T3). The FT-IR spectra of T1 composite of high % of BG showed the typical bands for BG structure with broadening in their bands. The band at 1090 cm^{-1} corresponds to the Si–O–Si asymmetric stretching mode, the band at 792 cm^{-1} is associated with a Si–O–Si symmetric stretching and the band at 476 cm^{-1} is assigned to the Si–O–Si symmetric bending mode and the shoulder at 950 cm^{-1} is related to the Si–O–Ca [14]. FT-IR spectrum of T1 composite showed that the bands at 596 and 603 cm^{-1} are associated with the stretching vibration of phosphate groups [15]. The spectra of T2 and T3 composites have the same behavior of T1 with broadening in the bands with some shift compared to original BG and titania. The intensity of Ti–O–Ti/Si–O–Si and/or PO_4^{3-} bands increased gradually as a result of the increase of titania content proving interaction between BG and titania forming Ca Ti (SiO_5) compound as in T3 composite containing the highest content of titania. This result coincided with the XRD data.

3.1.3. Mechanical testing

Table 2 shows the results of the compressive strength for T1, T2 and T3 composites. The results indicated that T3 composite had enhanced the mechanical results compared to T1 and T2 composites because of high content of titania into the T3 composite. Therefore, the T3 composite containing the highest content of titania (75%) resulted in a suitable compressive strength values that are comparable to the range of the human cortical bone [8]. In this domain, ceramic matrix biocomposites were reinforced by introducing another tough phase [8]. Therefore, BG material strengthened by adding titanium oxide and fired at 1000 °C to obtain BG/titania biocomposites having suitable mechanical properties.

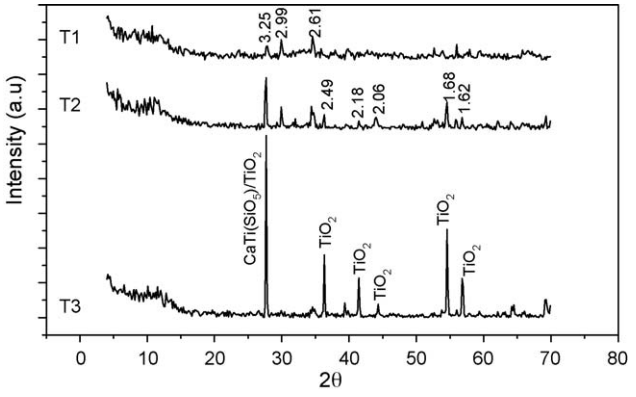

Fig. 1. X-ray diffraction of the prepared BG/titania composites.

3.2. Bioactivity behavior

3.2.1. Total calcium and phosphate ions

3.2.1.1. Total calcium ions (Ca^{2+}). The in vitro bioactivity result represents the possible change in Ca^{2+} and PO_4^{3-} ions concentration in SBF solution after soaking the samples for different periods. Fig. 3 shows lower levels of Ca^{2+} concentration for T1, T2 and T3 composites compared to control (control is SBF that contains ions similar to those in human blood plasma as previously in Table 2) at all periods proving the mineralization of calcium ions onto the composite surface at all periods. This result is in the favor of the formation of calcium phosphate layer and the T1 composite had higher ability to adsorb Ca^{2+} ions onto its surface compared to other composites proving effect of high content of BG into the composite on the deposition of calcium ions ().

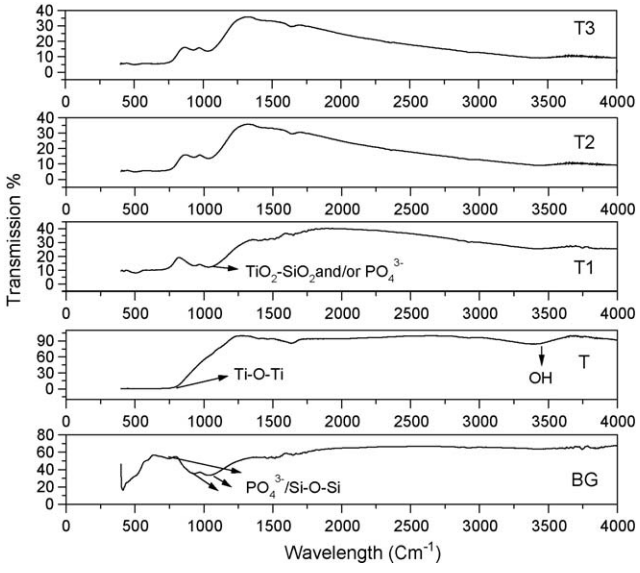

Fig. 2. FT-IR spectra of titania (T), bioactive glass (G), and their composites (T1, T2 and T3).

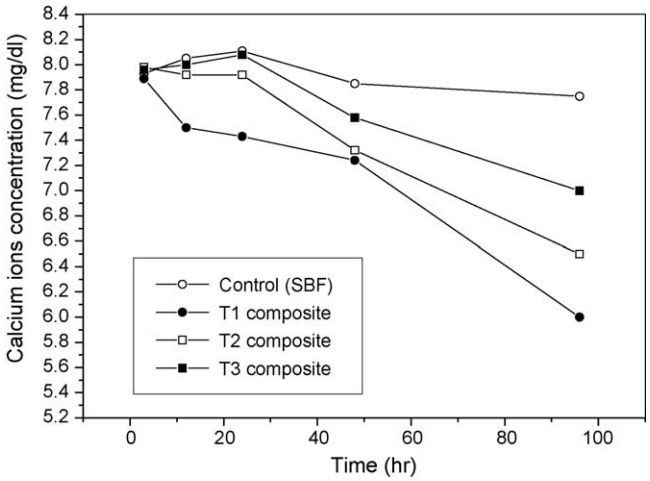

Fig. 3. Total calcium ions in SBF post-immersion of T1, T2 and T3 composites compared to control (SBF) and its standard deviation (%) for the tested samples ($n = 3$) is shown in Table 3.

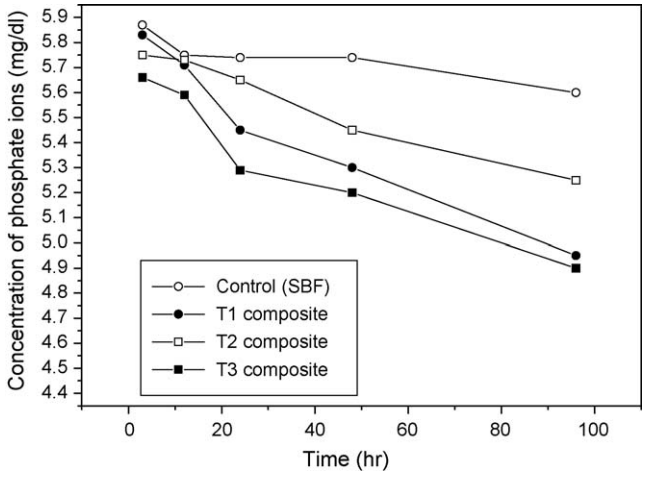

Fig. 4. Total phosphate ions in SBF post-immersion T1, T2 and T3 composites compared to control (SBF) and its standard deviation (%) for the tested samples ($n = 3$) is shown in Table 4.

3.2.1.2. Phosphate ions (PO_4^{3-}). Fig. 4 shows phosphate ions at different periods for the prepared BG/titania composites post-immersion in SBF. The PO_4^{3-} ions concentration at all periods records lower values for all composites compared to control denoting deposition of phosphate ions onto the composite surface especially T3 composite and after longer time. This result proves that the increase of titania content in the BG/titania composite results in high deposition of phosphate ions onto the composite surface, then this leads to the nucleation of apatite layer. The T2 composite material containing silica and titania into its structure in equal contents had high ability to form Si–OH and Ti–OH groups in SBF on the composite surface, then, it produces the competition between both groups to interact with phosphate ions compared to T1 and T3 composites containing high silica and titania contents, respectively, resulting to lowering deposition of phosphate ions. Therefore, the presence of titania and silica in high concentrations in BG/titania composites as in T1 and T3 composites, respectively, resulted in high contents of Si–OH and Ti–OH groups in both composites, respectively, leading to high facilitation of their interaction with phosphate ions onto the surface compared to T2 composite containing titania and silica with equal ratios (Fig. 4). This result is due to the presence of high content of Ti–OH or Si–OH groups into the media improved the interaction with phosphate ions onto the composite surface compared to their presence in the same concentration as the competition between two groups may reduce the interaction with phosphate ions to induce the apatite formation. Also, from Figs. 3 and 4, we notice that low deposition of calcium ions is accompanied with high deposition of phosphate ions onto the composite surface for T1, T2 and T3 BG/titania composites. This result is due to the release of calcium ions from the composite surface that is accompanied by deposition of phosphate ions on the same surface. Therefore, we coincided with who reported that there is an inverse relationship between deposition of calcium and phosphate ions onto the composite surface into the media [16] ().

3.2.2. FT-IR analysis

Figs. 5–7 show the corresponding FT-IR spectra of the three solid composites pre- and post-immersion in SBF for 4 days. Fig. 5 shows the intensity of phosphate and/or SiO_2–TiO_2 bands at 1030, 945 and 690 cm^{-1} as well as the appearance of new phosphate bands at 560, 470 and 440 cm^{-1} and carbonate band at 880 cm^{-1} in the spectrum of T1 composite post-immersion in SBF are enhanced compared to pre-immersion proving deposition of phosphate and carbonate ions onto the surface, then, this result is in favor of formation of carbonated apatite layer. In this domain, the presence of Si–OH and Ti–OH groups on composite surface resulted in apatite layer formation [4,7]. Fig. 6 shows the intensity of phosphate and/or SiO_2–TiO_2 bands at 1030 cm^{-1} post-immersion were enhanced compared to pre-immersion and the appearance of new bands such as carbonate at 888 cm^{-1} and bending phosphate at 670 and 550 cm^{-1}

Table 3
Standard errors (%) of total calcium ions concentration (Ca^{2+}) for the tested sample ($n = 3$).

	Period (h)				
	3	12	24	48	96
Control (SBF)	0.05	0.04	0.035	0.05	0.04
T1 composite	0.055	0.1	0.07	0.46	0.05
T2 composite	0.065	0.05	0.05	0.05	0.046
T3 composite	0.026	0.05	0.03	0.057	0.04

Table 4
Standard errors (%) of phosphate ions concentration (PO_4^{3-}) for the tested sample ($n = 3$).

	Period (h)				
	3	12	24	48	96
Control (SBF)	0.03	0.04	0.04	0.03	0.03
T1 composite	0.035	0.05	0.03	0.04	0.05
T2 composite	0.05	0.03	0.025	0.03	0.05
T3 composite	0.04	0.045	0.11	0.05	0.03

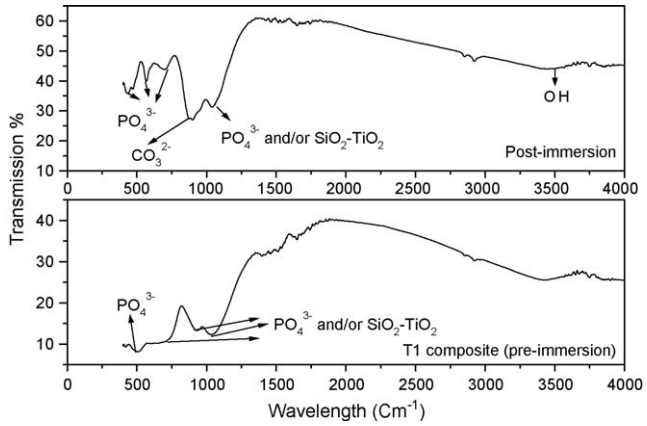

Fig. 5. The FT-IR of T1 composite pre- and post-immersion in SBF.

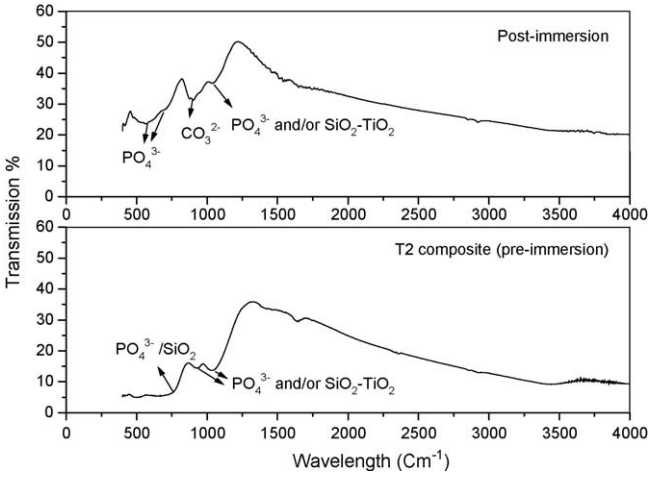

Fig. 6. The FT-IR of T2 composite pre- and post-immersion in SBF.

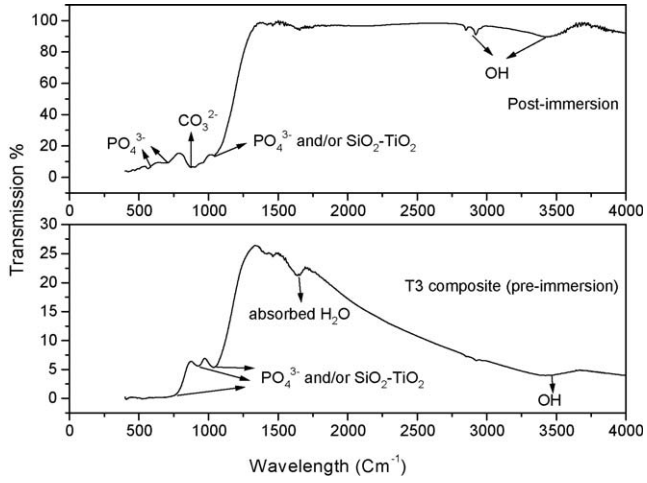

Fig. 7. The FT-IR of T2 composite pre- and post-immersion in SBF.

proving the formation of carbonated apatite layer. Fig. 7 shows the intensity of phosphate and/or SiO_2–TiO_2 bands at 1040 cm^{-1} post-immersion was enhanced compared to pre-immersion and the appearance of new bands such as carbonate at 882 cm^{-1} and bending phosphate at 700 and 560 cm^{-1} proving the formation of carbonated apatite layer. Therefore, the presence of abundant Ti–OH groups on the composite surface of T2 and T3 composites containing high content of titania compared to T1 composite resulted in the enhancement of apatite nucleation (Figs. 5–7).

3.2.3. Surface morphology

3.2.3.1. Pre-immersion in SBF. The SEM of the prepared biocomposites is shown in Fig. 8. The SEM (1000×) shows the morphology of the biocomposites surface pre-immersion and reveals the appearance of many rod shapes after addition of titania [17]. The SEM (Fig. 8a) of T1 composite containing high % of BG powder indicates the presence of grains of BG connected to each other and is characterized by fused structure including a round and oval grains resulting in high density of composite structure and proving some interaction between two phases. For T2 composite, SEM at the same magnification (Fig. 8b) indicates homogenous distribution of many grains having plate shapes characterizing calcium titanate or titania structure as well as the presence of minute particles distributed within these grains proving increase of interaction between two phases (BG and titania). The SEM at the same magnification (Fig. 8c) of T3 composite shows highly homogenous distribution of calcium titanate grains into the composite and appears blocky prismatic crystals perpendicular with additional phase of thick interlocked platelet shaped crystals in parallel view proving effect of high titania content at the expense of BG powder.

3.2.3.2. Post-immersion in SBF. The glass releases Ca^{2+} and Na^{+} ions from its surface via an exchange with the H_3O^{+} ion in the SBF to form Si–OH or Ti–OH groups on their surfaces [2]. Water molecules in the SBF simultaneously react with the Si–O–Si or Ti–O–Ti bond to form additional Si–OH or Ti–OH groups, the formed Si–OH and Ti–OH groups induce apatite nucleation, and the released Ca^{2+} and Na^{+} ions accelerate apatite nucleation by increasing the ionic activity product of apatite in the fluid [8]. As a result, the apatite layer forms onto the composite surface after soaking in SBF in a short period (4 days) and this phenomenon is confirmed by SEM of BG/titania composites post-immersion as shown in Fig. 8d–f.

For T1 biocomposites, SEM at 500× (Fig. 8d) shows that this composite has many particles on its surface proving slight formation of apatite layer due to the composite contains high content of silica characterizing melted and dense structure that reduced nucleation of apatite layer compared to other composites. In this domain, the simultaneous dissolution of silicates results in the formation of silanol groups on material's surface, which are essential for nucleation sites resulting in HA formation [4]. Once the apatite nuclei formed, they can grow spontaneously by consuming the calcium phosphate ions in the surrounding fluid [18]. For T2 and T3 composites, SEM at the same magnification (500×) indicates the presence of abundant spherical shapes with their accumulation on each other to form a bone-like apatite layer for both composites especially T3 composites. This result is due to T3 composites contains high content of titania which leads to increase of Ti–OH groups at the expense of Si–OH groups resulting in high nucleation of

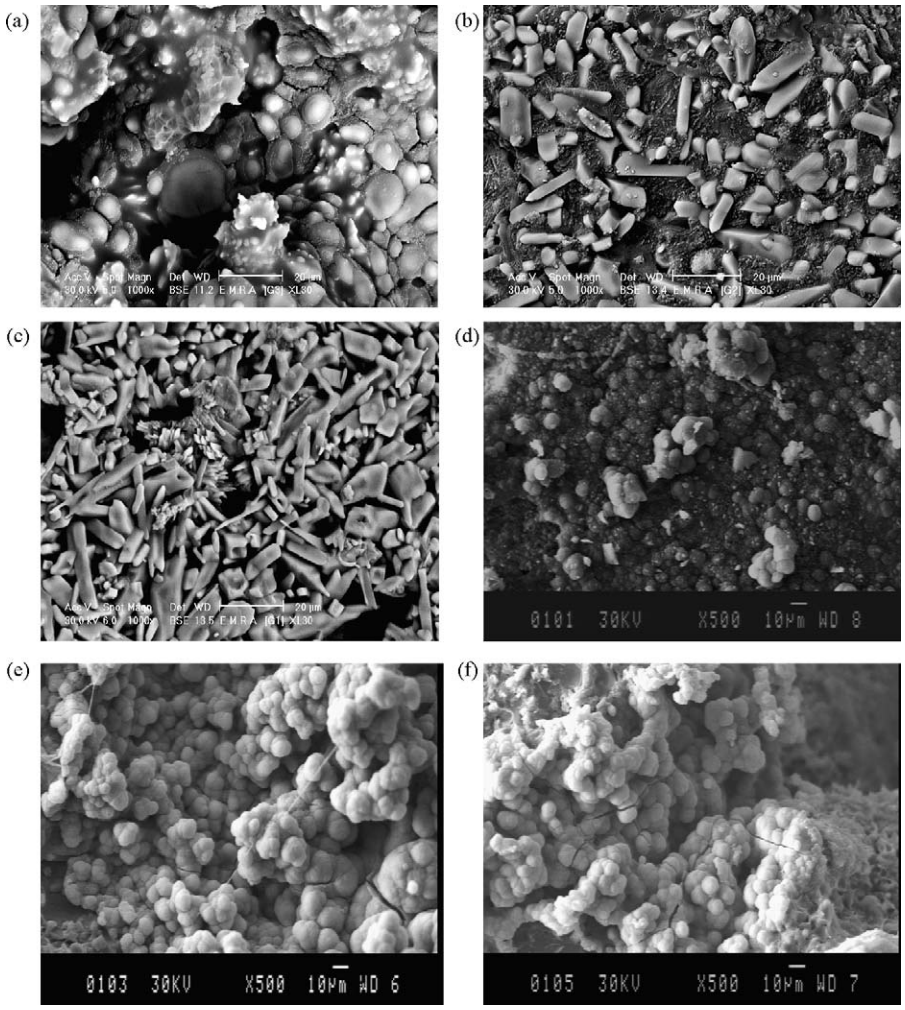

Fig. 8. (a), (b) and (c) SEM of the BG/titania composites for T1, T2 and T3 composites pre-immersion, respectively, and (d), (e) and (f) for T1, T2 and T3 composites post-immersion, respectively.

apatite (Fig. 8e and f). In this study, we noted that the rutile form of titania is the main phase in three composites and is essential for improvement of apatite nucleation especially T2 and T3 composites compared to T1 composites containing low content of titania. The catalytic effect of the Si–OH groups and Ti–OH groups for the apatite nucleation has proven by the observation that silica and titanium will form apatite on their surfaces in SBF and are abundant on the composite surfaces [4,7,19]. Also, as it was reported that the anatase crystal plays an important role in the apatite formation in SBF [20]. Therefore, we noted that the presence of rutile titania form into the BG/titania composites especially T3 composite containing high content of rutile in its structure enhanced its ability to induce the formation of apatite layer as shown by XRD, SEM, in vitro and FT-IR data pre- and post-immersion.

4. Conclusion

The phase and FT-IR analyses confirmed the interaction between BG and titania (anatase) forming calcium titanium silicate and rutile compounds. The data proved that the increase titania content into the composite improved the mechanical properties as in T3 composite having the highest content of titania powder. It is noted that T3 composite had compressive strength (122.31 MPa) comparable to that of the cortical bone that is located in the range of 100–230 MPa. Bioactivity results indicated that T2 and T3 composites containing high content of titania resulting in the abundance of Ti–OH groups on the composite surface had an enhanced ability to form the bone-like apatite layer compared to T1 composite having high content of BG characterizing dense structure. Additionally, the formed rutile titania in these biocomposites had the ability to induce the formation of carbonated apatite layer comparable to anatase form. Thus, these biocomposite materials are promising for medical applications such as bone substitutes especially in load-bearing sites.

References

[1] D.J. Berry, W.D. Harmsen, M.E. Cabanela, M.F. Morrey, J. Bone Joint Surg. (Am) 84A (2) (2002) 171–177.
[2] L.L. Hench, The discovery of bioactive glasses, in: Science Faith and Ethics, Imperial College Press, London, 2001.
[3] T. Kokubo, H.M. Kim, M. Kawashita, T. Nakamura, J. Aust. Ceram. Soc. 36 (2000) 37–46.

[4] K.H. Karlsson, Glass Technol. 45 (2004) 157–161.
[5] C. Yuron, Z. Lian, J. Mater. Chem. Phys. 94 (2005) 283–287.
[6] I.B. de Arenas, C. Schattner, M. Vásquez, Ceram. Int. 32 (5) (2006) 515–520.
[7] C. Ohtsuki, H. Iida, S. Nakamura, A. Osaka, J. Biomed. Mater. Res. 35 (1997) 39.
[8] T. Kokubo, H. Kim, M. Kawashita, Biomaterials 24 (2003) 2161–2175.
[9] H. Oonishi, L.L. Hench, J. Wilson, F. Sugihara, M. Matsuura, S. Mizokawa, J. Biomed. Mater. Res. 51 (2000).
[10] T. Kokubo, F. Miyaji, H.M. Kim, T. NaKamura, J. Am. Ceram. Soc. 79 (1996) 1127–1129.
[11] C. Ohtsuki, Y. Aoki, T. Kokubo, Y. Bando, M. Neo, T. Nakamura, J. Ceram. Soc. Jpn. 103 (1995) 449–454.
[12] C.C. Wang, J.Y. Ying, Chem. Mater. 11 (11) (1999) 3113–3120.
[13] H.M. Kim, F. Miyaji, T. Kokubo, M. Kobayashi, T. Nakamura, Bull. Chem. Soc. Jpn. 69 (1996) 2387–2394.
[14] M.M. Perira, A.E.C. Hench, Calcium phosphate formation on sol–gel galsses in vitro., Studies Inorganic Chemistry, vol. 18, Elsevier, Amsterdam, 1994, p. 59.
[15] J.C. Elliott, Structure and chemistry of the apatite and other calcium orthophosphate., Studies Inorganic Chemistry, vol. 18, Elsevier, Amsterdam, 1994, p. 59.
[16] N. Spanos, P.G. Koutsoukos, J. Mater. Sci. 36 (2001) 573–578.
[17] M. Sato, M.A. Sambito, A. Aslani, N.M. Kalkhoran, E.B. Slamovich, T.J. Webster, Biomaterials 27 (2006) 2358–2369.
[18] Y. Ebisawa, T. Kokubo, K. Ohura, T. Yamamuro, J. Mater. Sci. Mater. Med. 1 (1993) 239–244.
[19] P. Li, C. Ohtsuki, T. Kokubo, K. Nakanishi, N. Soga, T. Nakamura, K.A. de Groot, J. Biomed. Mater. Res. 28 (1994) 7–15.
[20] H. Maeda, T. Kasuga, M. Nogami, J. Eur. Ceram. Soc. 24 (2004) 2125–2130.